Probing the $[CoC_2H_6]^+$ Potential Energy Surface: A Detailed Guided-Ion Beam Study

Chris L. Haynes, Ellen R. Fisher,† and P. B. Armentrout*

Contribution from the Department of Chemistry, University of Utah, Salt Lake City, Utah 84112

Received November 9, 1995⊗

Abstract: The potential energy surface for the $CoC_2H_6^+$ system is probed by using a guided-ion beam tandem mass spectrometer in conjunction with a dc discharge/flow tube ion source. Bimolecular reactions of $Co^+ + C_2H_6$, $Co^+(C_2H_4) + H_2$ (D_2), and $CoCH_2^+ + CH_4$ (CD_4) are examined, as well as threshold collisional activation of $Co^+(C_2H_6)$ and $Co^+(C_2H_4)$ with Xe. The results allow details of the $[CoC_2H_6]^+$ potential energy surface (PES) to be elucidated. Key features of the PES include barrier heights of 1.04 ± 0.11 eV (0.29 ± 0.09 eV in excess of the endothermicity) for the reaction of Co^+ with ethane to form $CoCH_2^+ + CH_4$ and of 0.32 ± 0.12 eV for the exothermic reaction to form $Co^+(C_2H_4) + H_2$. From the collisional activation studies, we determine 0 K bond dissociation energies for $Co^+-C_2H_4$ and $Co^+-C_2H_6$ complexes of 1.86 ± 0.07 and 1.04 ± 0.05 eV, respectively, in good agreement with literature values. $D_0(DCo^+-C_2H_4) = 1.13 \pm 0.16$ eV is also determined although it is somewhat more speculative.

Introduction

C−C and C−H bond activation in saturated and unsaturated hydrocarbons by transition metal ions has undergone considerable research.[1,2] In particular, Co^+ has been studied intensely in part because the valence electron configuration of its ^3F ground state ($3d^8$) has an empty 4s orbital allowing efficient reactivity. Experimentally, such studies include ion beam studies of the bimolecular reactions of Co^+ with methane,[3] ethane,[3,4] propane,[3−6] deuterated propanes,[7] and alkenes,[8−10] in addition to reaction rate studies of these systems at thermal energies.[1,11,12] Recent work includes studies of Co^+−alkane complexes[13] and reactions of electronic state specific cobalt ions with propane.[14] Theoretical studies include several products of the $Co^+ + C_2H_6$ reaction, e.g., CoH^+,[15−18] $CoCH_2^+$,[17−20] $CoCH_3^+$,[17,18,21] $CoC_2H_4^+$,[17,18,22] the $Co(CH_3)_2^+$ intermediate,[18,23,24] and the complexation of Co^+ with small alkanes.[25] Recently, details of the $[CoC_2H_6]^+$ potential energy surface (PES) have been calculated.[17,18]

Scheme 1

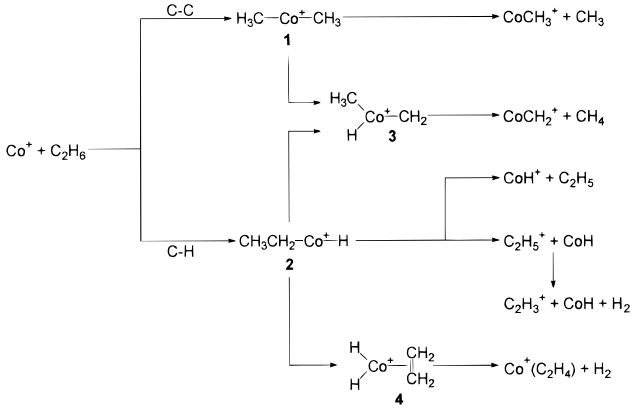

The various products observed in the reaction of Co^+ with ethane are shown in Scheme 1, which reproduces the mechanism suggested previously.[3] The theoretical calculations of Perry[17] and those of Holthausen and Koch (HK)[18] agree that the initial step in the dehydrogenation reaction to form $Co^+(C_2H_4) + H_2$ is C−H bond activation to form intermediate **2**, $H-Co^+-C_2H_5$.

† Department of Chemistry, Colorado State University, Fort Collins, CO 80523.

⊗ Abstract published in *Advance ACS Abstracts,* March 15, 1996.

(1) Allison, J. *Prog. Inorg. Chem.* **1986**, *34*, 627. Squires, R. R. *Chem. Rev.* **1987**, *87*, 623. *Gas Phase Inorganic Chemistry*, Russell, D. H., Ed.; Plenum: New York, 1989. Eller, K.; Schwarz, H. *Chem. Rev.* **1991**, *91*, 1121. Weisshaar, J. C. *Adv. Chem. Phys.* **1992**, *82*, 213. van Koppen, P. A. M.; Kemper, P. R.; Bowers, M. T. *Organometallic Ion Chemistry*, Freiser, B. S., Ed.; Kluwer: Dordrecht, 1995; p 157.

(2) Armentrout, P. B. In *Selective Hydrocarbon Activation: Principles and Progress*; Davies, J. A., Watson, P. L., Liebman, J. F., Greenberg, A., Eds.; VCH: New York, 1990; pp 467−533.

(3) Armentrout, P. B.; Beauchamp, J. L. *J. Am. Chem. Soc.* **1981**, *103*, 784.

(4) Georgiadis, R.; Fisher, E. R.; Armentrout, P. B. *J. Am. Chem. Soc.* **1989**, *111*, 4251.

(5) Houriet, R.; Halle, L. F.; Beauchamp, J. L. *Organometallics* **1983**, *2*, 1818.

(6) van Koppen, P. A. M.; Brodbelt-Lustig, J.; Bowers, M. T.; Dearden, D. V.; Beauchamp, J. L.; Fisher, E. R.; Armentrout, P. B. *J. Am. Chem. Soc.* **1990**, *112*, 5664.

(7) van Koppen, P. A. M.; Brodbelt-Lustig, J.; Bowers, M. T.; Dearden, D. V.; Beauchamp, J. L.; Fisher, E. R.; Armentrout, P. B. *J. Am. Chem. Soc.* **1991**, *113*, 2359.

(8) Armentrout, P. B.; Beauchamp, J. L. *J. Chem. Phys.* **1981**, *74*, 2819.

(9) Armentrout, P. B.; Halle, L. F.; Beauchamp, J. L. *J. Am. Chem. Soc.* **1981**, *103*, 6624.

(10) Haynes, C. L.; Armentrout, P. B. *Organometallics* **1994**, *13*, 3480.

(11) Jacobson, D. B.; Freiser, B. S. *J. Am. Chem. Soc.* **1983**, *105*, 5197.

(12) Tonkyn, R.; Ronan, M.; Weisshaar, J. C. *J. Phys. Chem.* **1988**, *92*, 92.

(13) Kemper, P. R.; Bushnell, J.; van Koppen, P.; Bowers, M. T. *J. Phys. Chem.*, **1993**, *97*, 1810.

(14) van Koppen, P. A. M.; Kemper, P. R.; Bowers, M. T. *J. Am. Chem. Soc.* **1995**, *117*, 10941.

(15) Schilling, J. B.; Goddard, W. A., III; Beauchamp, J. L. *J. Am. Chem. Soc.* **1986**, *108*, 582.

(16) Pettersson, L. G. M.; Bauschlicher, C. W., Jr.; Langhoff, S. R.; Partridge, H. *J. Chem. Phys.* **1987**, *87*, 481.

(17) Perry, J. K. Ph.D. Thesis, Caltech, 1994.

(18) Holthausen, M. C.; Koch, W. Work in progress

(19) Bauschlicher, C. W., Jr.; Partridge, H.; Sheehy, J. A.; Langhoff, S. R.; Rosi, M. *J. Phys. Chem.* **1992**, *96*, 6969.

(20) Musaev, D. G.; Morokuma, K.; Koga, N.; Nguyen, K. A.; Gordon, M. S.; Cundari, T. R. *J. Phys. Chem.* **1993**, *97*, 11435.

(21) Bauschlicher, C. W., Jr.; Langhoff, S. R.; Partridge, H.; Barnes, L. A. *J. Chem. Phys.* **1989**, *91*, 2399.

(22) Sodupe, M.; Bauschlicher, C. W.; Langhoff, S. R.; Partridge, H. *J. Phys. Chem.* **1992**, *96*, 2118.

(23) Perry, J. K.; Goddard, W. A., III; Ohanessian, G. *J. Chem. Phys.* **1992**, *97*, 7560.

(24) Rosi, M.; Bauschlicher, C. W., Jr.; Langhoff, S. R.; Partridge, H. *J. Phys. Chem.* **1990**, *94*, 8656.

(25) Perry, J. K.; Ohanessian, G.; Goddard, W. A. *J. Phys. Chem.* **1993**, *97*, 5238.

0002-7863/96/1518-3269$12.00/0

In contrast to Scheme 1, the studies of both Perry and HK show that the $H_2Co^+(C_2H_4)$ dihydride intermediate **4** is unstable. Instead, dehydrogenation occurs by a concerted mechanism leading directly to $(H_2)Co^+(C_2H_4)$. These studies find a barrier for the exothermic dehydrogenation reaction, in agreement with previous experimental studies.[4] Although Perry did not carry out calculations concerning the pathways available for C−C bond activation of ethane by Co^+, the work of HK does include this. They find that intermediate **1** loses CH_4 through a four-centered transition state rather than involving intermediate **3**. This process is analogous to that described experimentally and theoretically for the dehydrogenation of methane by Co^+.[20,26]

In the present experiments, several reactions are used to probe the $[CoC_2H_6]^+$ PES in order to gain further insight into the ability of Co^+ to activate C−C and C−H bonds and to compare to the theoretical calculations. Specifically, we reexamine the $Co^+ + C_2H_6$ system with higher sensitivity, study several bimolecular reactions, $Co^+(C_2H_4) + H_2$ (D_2) and $CoCH_2^+ + CH_4$ (CD_4), and use threshold collision activation[10,27−30] (TCA) to characterize the $Co^+(C_2H_6)$ intermediate. These various means of entering the $[CoC_2H_6]^+$ PES allow us to obtain information on the energies of intermediates and transition states along the PES.

Experimental Section

The guided-ion beam instrument on which these experiments were performed has been described in detail previously.[31,32] Ions are created in a flow tube source as described below, extracted from the source, accelerated, and passed through a magnetic sector for mass analysis. The mass-selected ions are decelerated to the desired kinetic energy and focused into an octopole ion beam guide. This device uses radio-frequency electric fields to trap the ions in the radial direction and ensure complete collection of reactant and product ions. The octopole passes through a gas cell with an effective length of 8.26 cm that contains the neutral collision partner at a pressure sufficiently low that multiple ion−molecule collisions are improbable. Except for two products in the $Co^+ + C_2H_6$ reaction (specified below), it was verified that the results presented here exhibit no dependence on pressure and thus correspond to single ion−molecule collisions. The unreacted parent and product ions drift to the end of the octopole from which they are extracted, pass through a quadrupole mass filter for mass analysis, and are detected with a secondary electron scintillation ion detector using standard pulse counting techniques. Raw ion intensities are converted to cross sections as described previously.[31] We estimate absolute cross sections to be accurate to ±20%.

Laboratory (lab) energies are converted to energies in the center of mass (CM) frame by using $E_{CM} = E_{lab}M/(M + m)$, where m and M are the ion and neutral masses, respectively. The absolute energy scale and corresponding full width at half maximum (fwhm) of the ion beam kinetic energy distribution are determined by using the octopole as a retarding energy analyzer as described previously.[31] The absolute uncertainty in the energy scale is ±0.05 eV (lab). The energy distributions in these studies are nearly Gaussian and have a typical fwhm of 0.2−0.5 eV (lab).

Co^+ ions are produced by using a direct current discharge source[28] consisting of a cobalt cathode held at high negative voltage (1.5−3 kV) over which a flow of approximately 90% He and 10% Ar passes. Ar^+ ions created in the discharge are accelerated toward the cobalt cathode, sputtering off ionic and neutral metal atoms. If required, an appropriate source gas is added to the flow about 60 cm downstream of the discharge. For production of Co^+, about 1−3 mTorr of CH_4 is added to quench excited states. Under these conditions, we have found that the Co^+ ions have an electron state distribution characterized by a temperature of 800 ± 100 K.[10] To form $Co^+(C_2H_6)$ and $Co^+(C_2H_4)$, we add either ethane or ethene, respectively, to the flow gases such that the desired complexes are formed by three-body collisions. $CoCH_2^+$ ions are generated by bimolecular reaction of Co^+ ions with ethylene oxide added to the flow.[10,26] At typical flow tube pressures of 0.5−0.6 Torr, the ions undergo $>10^4$ thermalizing collisions as they traverse the remaining 40 cm of the flow tube. Ions are extracted from the flow tube and gently focused through a 9.5 cm long differentially pumped region before entering the rest of the instrument described above. Before any experimental run, a high-energy (20−25 eV, lab) collision-induced dissociation (CID) spectrum with Xe was taken in order to make sure that no impurity ions were present in the parent ion beam. CID of the $CoCH_2^+$ beam revealed only a Co^+ product with a threshold consistent with previously determined thermochemistry of $CoCH_2^+$.[33]

Thermochemical Analysis. Cross sections are modeled by using eq 1,[28,34]

$$\sigma = \sigma_0 \sum_i g_i (E + E_i + E_{rot} - E_0)^n / E \qquad (1)$$

where E is the relative translational energy, E_0 is the reaction threshold at 0 K, σ_0 is an energy-independent scaling parameter, and the exponent n is treated as a variable parameter. E_{rot} is the average rotational energies of the reactants at 300 K: 0.039 eV $= 3k_BT/2$ for $Co^+ + C_2H_6$, $CoC_2H_6^+ + Xe$, and $CoC_2H_4^+ + Xe$; 0.065 eV $= 5k_BT/2$ for $CoC_2H_4^+ + H_2$; and 0.078 eV $= 3k_BT$ for $CoCH_2^+ + CH_4$. Vibrational energies of the polyatomic reactants are included explicitly in eq 1 as a summation over vibrational energy levels, i, with energies E_i and relative populations g_i ($\Sigma g_i = 1$). We use the Beyer−Swinehart algorithm[35] to calculate a Maxwell−Boltzmann distribution of vibrational energies at 300 K which is used for the factors g_i in eq 1. We have described this modeling procedure in detail elsewhere.[28]

The vibrational frequencies used for the polyatomic reactants are given in Table 1. The vibrational energy contributions from H_2 and D_2 are negligible and those for CH_4 (0.001 eV), CD_4 (0.0012 eV), and C_2H_6 (0.019 eV) are sufficiently small that the average vibrational energy is used rather than the explicit sum. For the $Co^+(C_2H_x)$ complexes, several sets of values for the modes involving Co^+ are listed and span the limits of what is reasonable. Because these species have few low-frequency modes, the average vibrational energies for $CoCH_2^+$, $Co^+(C_2H_4)$, and $Co^+(C_2H_6)$ at 300 K are only 0.015, 0.036, and 0.049 eV, respectively. Therefore, the exact choice of vibrational frequencies is not critical to the thermochemistry determined here. In the case of the $Co^+ + C_2H_6$ reaction, the thresholds are modeled assuming that 99.66% of the Co^+ ions are in the a^3F ground state and 0.34% are in the a^5F first excited state, corresponding to a temperature of 800 K, as determined in previous experiments.[10] We assume that the populations of any electronic states of the polyatomic ions have equilibrated to the temperature of the flow gas, 300 K, such that the average electronic energy is negligible. Even if the distribution is somewhat hotter, it is unlikely that the contributions of electronic excitation will influence the thresholds determined here outside the error limits provided.

Hydrocarbon gases were obtained from Matheson in high purity (>99%) and used without further purification. Xenon (99.995%, Air Products) was used without further purification, except for multiple freeze−pump−thaw cycles to remove noncondensible impurities.

Results

In the presentation below, representative results for the various reactions examined are provided. Thermochemistry at 0 K is

(26) Haynes, C. L.; Chen, Y.-M.; Armentrout, P. B. *J. Phys. Chem.* **1995**, *99*, 9110.
(27) Schultz, R. H.; Armentrout, P. B. *Organometallics* **1992**, *11*, 828.
(28) Schultz, R. H.; Crellin, K. C.; Armentrout, P. B. *J. Am. Chem. Soc.* **1991**, *113*, 8590.
(29) Schultz, R. H.; Armentrout, P. B. *J. Phys. Chem.* **1992**, *96*, 1662.
(30) Schultz, R. H.; Armentrout, P. B. *J. Am. Chem. Soc.* **1991**, *113*, 729.
(31) Ervin, K. M.; Armentrout, P. B. *J. Chem. Phys.* **1985**, *83*, 166.
(32) Schultz, R. H.; Armentrout, P. B. *Int. J. Mass Spectrom. Ion Processes* **1991**, *107*, 29.
(33) Armentrout, P. B.; Kickel, B. L. In *Organometallic Ion Chemistry*; Freiser, B. S., Ed.; Kluwer: Dordrecht, 1995; pp 1−45.
(34) Armentrout, P. B. In *Advances in Gas Phase Ion Chemistry*; Adams, N. G., Babcock, L. M., Eds.; JAI: Greenwich, 1992; Vol. 1, pp 83−119.
(35) Beyer, T.; Swinehart, D. F. *Comm. Ass. Comput. Machines* **1973**, *16*, 379. Stein, S. E.; Rabinovitch, B. S. *J. Chem. Phys.* **1973**, *58*, 2438. Stein, S. E.; Rabinovitch, B. S. *Chem. Phys. Lett.* **1977**, *49*, 183. Gilbert, R. G.; Smith, S. C. *Theory of Unimolecular and Recombination Reactions*, Blackwell Scientific Publications: Oxford, 1990.

Table 1. Vibrational Frequencies (in cm^{-1})[a]

species	frequencies
H_2[b]	4401.2
CH_4[c]	1306(3), 1534(2), 2916.5, 3018.7(3)
C_2H_4[d]	826, 943, 949, 1023, 1236, 1342, 1444, 1623, 2989, 3026, 3103, 3106
C_2H_6[d]	289, 822(2), 995, 1190(2), 1379, 1388, 1468(2), 1469(2), 2896, 2954, 2969(2), 2985(2)
$Co^+(C_2H_4)$	A: ethene + 100, 300, 500
	B: ethene + 100, 400, 700
	C: ethene + 300, 500, 700
$Co^+(C_2H_6)$	A: ethane + 100, 300, 500
	B: ethane + 100, 400, 700
	C: ethane + 300, 500, 700
$CoCH_2^+$[e]	452, 624, 700, 1319, 2942, 3012

[a] Degeneracies in parentheses. [b] Huber, K. P.; Herzberg, G. In *Molecular Spectra and Molecular Structure. IV. Constants of Diatomic Molecules*; Van Nostrand Reinhold: New York, 1979. [c] Chase, M. W., Jr.; Davies, C. A.; Downey, J. R., Jr.; Frurip, D. J.; McDonald, R. A.; Syverud, A. N. *J. Phys. Chem. Ref. Data* **1985**. *14*, No. 1 (JANAF Tables). [d] Shimanouchi, T. *Tables of Molecular Vibrational Frequencies*; National Bureau of Standards: Washington, DC, 1972; Consolidated Vol. I. [e] Vibrational frequencies are assumed to equal those for $FeCH_2$ and are taken from: Hauge, R. H.; Margrave, J. L.; Kafafi, Z. H. In *Chemistry and Physics of Matrix-Isolated Species*; Andrews, L., Moskovits, M., Eds.; North-Holland: Amsterdam, 1989; p 289.

indicated with each reaction and is determined from literature information given in Tables 2 and 3. For simplicity, the values given are for perprotio species in all cases, thereby neglecting the zero point energy differences for deuterated species. The cross sections of each product are analyzed with eq 1, and the optimum parameters obtained are listed in Table 4. In all reaction systems studied here, about five data sets are analyzed in each case. For most reactions, the data sets were collected over a two to three year period.

$Co^+ + C_2H_6$. Results for the reaction of $Co^+ + C_2H_6$ are shown in Figure 1. We observe nine products corresponding to reactions 2−10.

$$Co^+ + C_2H_6 \rightarrow CoC_2H_6^+ + 1.21 \pm 0.07 \text{ eV} \quad (2)$$

$$\rightarrow CoC_2H_4^+ + H_2 + 0.48 \pm 0.22 \text{ eV} \quad (3)$$

$$\rightarrow CoCH_3^+ + CH_3 - 1.71 \pm 0.04 \text{ eV} \quad (4)$$

$$\rightarrow CoCH_2^+ + CH_4 - 0.75 \pm 0.06 \text{ eV} \quad (5)$$

$$\rightarrow CoCH^+ + CH_3 + H_2 - 4.05 \pm 0.38 \text{ eV} \quad (6)$$

$$\rightarrow CoC^+ + CH_4 + H_2 - 3.79 \pm 0.30 \text{ eV} \quad (7)$$

$$\rightarrow CoH^+ + C_2H_5 - 2.33 \pm 0.06 \text{ eV} \quad (8)$$

$$\rightarrow C_2H_5^+ + CoH - 2.70 \pm 0.07 \text{ eV} \quad (9)$$

$$\rightarrow C_2H_3^+ + CoH + H_2 - 4.84 \pm 0.08 \text{ eV} \quad (10)$$

Results for reaction 2 are not shown in Figure 1 because the cross section for the $CoC_2H_6^+$ product was found to be linearly dependent on the C_2H_6 reactant pressure. This indicates that this adduct ion is formed by termolecular stabilization. All other

Table 2. Literature Thermochemistry (in kJ/mol)

species	$\Delta_f H°_0$	species	$\Delta_f H°_0$
H	216.035 ± 0.006[a]	C_2H_2	288.8 ± 0.7[c,f]
C	711.2 ± 0.5[a]	C_2H_4	61.0 ± 0.4[c,f]
CH	592.9 ± 1.7[b]	C_2H_5	132.2 ± 2.1[e]
CH_2	388.3 ± 2.5[c,d]	$C_2H_5^+$	915.2 ± 2.3[e]
CH_3	149.8 ± 0.4[c,e]	C_2H_6	-68.2 ± 0.4[c,f]
CH_4	-66.4 ± 0.4[c,f]	Co	425.1 ± 2.1[a]
		Co^+	1183.9 ± 2.1[a]

[a] Footnote *c* of Table 1. [b] Ervin, K. M.; Gronert, S.; Barlow, S. E.; Gilles, M. K.; Harrison, A. G.; Bierbaum, V. M.; DePuy, C. H.; Lineberger, W. C.; Ellison, G. B. *J. Am. Chem. Soc*. **1990**, *112*, 5750. [c] Converted from $\Delta_f H°_{298}$ given using information in footnote *a*. [d] Leopold, D. G.; Murray, K. K.; Stevens Miller, A. E.; Lineberger, W. C. *J. Chem. Phys*. **1985**, *83*, 4849. [e] Reference 36. [f] Pedley, J. B.; Naylor, R. D.; Kirby, S. P. *Thermochemical Data of Organic Compounds*, 2nd ed.; **1986**, Chapman and Hall: New York, 1986.

Table 3. Cobalt−Ligand Bond Dissociation Energies (in eV) at 0 K

species	experiment	theory
Co^+-H	1.98 ± 0.06[a]	
Co^+-D	2.01 ± 0.06[b]	
Co−H	1.86 ± 0.05[a]	
Co^+-H_2	0.79 ± 0.04,[c] 0.76 ± 0.10[d]	
Co^+-C	3.60 ± 0.30[e]	
Co^+-CH	4.35 ± 0.38[e]	
Co^+-CH_2	3.29 ± 0.05[a]	
Co^+-CH_3	2.10 ± 0.04[a]	
Co^+-CH_4	0.93 ± 0.06,[f] 0.99 ± 0.03[c]	
$Co^+-C_2H_2$	$\geq 0.28 \pm 0.13$[g]	1.72[h]
$Co^+-C_2H_4$	1.86 ± 0.07,[i] 1.82 ± 0.22,[j] $> 1.73 \pm 0.28$[m]	1.51,[k] 1.88,[l] 2.14[n]
$Co^+-C_2H_5$	$> 1.76 \pm 0.09$,[o] 2.00 ± 0.11[a]	1.96,[p] 2.43[q]
$DCo^+-C_2H_4$	1.13 ± 0.16[i]	
$Co^+-C_2H_6$	1.04 ± 0.05,[i] 1.21 ± 0.07[c]	1.06,[r] 1.23[s]
Co^+-Xe	0.85 ± 0.07[f]	
$(CH_2)Co^+-H_2$		0.36[t]
$(C_2H_4)Co^+-D$	1.28 ± 0.13[i]	
$(C_2H_4)Co^+-H_2$		0.74,[p] 0.69[q]

[a] Reference 33. [b] Elkind, J. L.; Armentrout, P. B. *J. Phys. Chem*. **1986**, *90*, 6576. [c] Reference 13. [d] Reference 53. [e] Reference 26. [f] Haynes, C. L.; Armentrout, P. B.; Perry, J. K.; Goddard, W. A., III *J. Phys. Chem*. **1995**, *99*, 6340. [g] Reference 10. [h] $D(Co^+-C_2H_2)$ is estimated in ref 10 from a D_e value of 1.44 eV in: Sodupe, M.; Bauschlicher, C. W. *J. Phys. Chem*. **1991**, *95*, 8640. [i] This work. [j] Reference 42. [k] Reference 22, converted from D_e values as described in text. [l] Reference 17, converted from D_e values as described in text. [m] Reference 41, 298 K. [n] Reference 18, converted from a D_e value of 2.21 eV, see text. [o] Reference 43. [p] Reference 17. [q] D_e value from ref 18. [r] Reference 25. [s] Reference 18, converted from a D_e value of 1.26 eV see text. [t] D_e value taken from ref 20.

product cross sections were found to be pressure independent except for the second feature on the $CoC_2H_4^+$ product observed at about 6 eV. This feature has a small pressure dependence, although the cross section does not disappear upon extrapolation to zero pressure (single collision) conditions. $CoC_2H_5^+$ and $CoC_2H_2^+$ products were looked for but not observed in this reaction system, indicating cross sections less than 10^{-18} cm^2.

The present results are consistent with previous ion beam studies of Armentrout and Beauchamp (AB)[3] and Georgiadis, Fisher, and Armentrout (GFA).[4] In both previous studies, the CoH^+ and $CoCH_3^+$ ions are the major products observed and have similar maximum cross sections to each other and to the absolute cross sections observed here. GFA also observed the $C_2H_5^+$ product. AB did not, presumably because this slow product is not efficiently collected by the instrument used (which had no octopole). The minor products, $CoC_2H_4^+$ and $CoCH_2^+$, were observed by both AB and GFA, although the small intensity of these species prevented extraction of any detailed information from them. GFA also had difficulties resolving

Table 4. Parameters Used in Eq 1 for Fitting Reaction Cross Sections

product	n	σ_0	E_0, eV	E_0, eV (lit.)[a]
		$Co^+ + C_2H_6$		
CoH^+	1.4 ± 0.1	2.8 ± 0.3	2.36 ± 0.10	2.33 ± 0.06
$CoCH^+$	2.6 ± 0.4	0.02 ± 0.01	4.86 ± 0.51	4.05 ± 0.38
$CoCH_2^+$	2.9 ± 0.6	0.14 ± 0.20	1.11 ± 0.22	0.75 ± 0.06
$CoCH_3^+$	1.8 ± 0.3	3.6 ± 0.7	1.84 ± 0.10	1.71 ± 0.04
$CoC_2H_4^+$	3.4 ± 0.4	0.03 ± 0.01	0.32 ± 0.12	-0.48 ± 0.22
$C_2H_3^+$	1.0 ± 0.2	0.60 ± 0.09	4.77 ± 0.12	4.84 ± 0.08
$C_2H_5^+$	1.3 ± 0.2	1.1 ± 0.2	2.65 ± 0.09	2.70 ± 0.07
		$CoC_2H_6^+ + Xe$		
Co^+	1.5 ± 0.1	9.31 ± 0.62	1.04 ± 0.05	1.21 ± 0.07
CoH^+	1.7 ± 0.4	0.20 ± 0.10	4.09 ± 0.46	3.54 ± 0.09
$CoCH_3^+$	1.6 ± 0.6	0.29 ± 0.21	3.80 ± 0.20	2.92 ± 0.08
		$CoC_2H_4^+ + Xe$		
Co^+	1.7 ± 0.1	2.30 ± 0.19	1.86 ± 0.07	1.82 ± 0.22
$CoXe^+$	2.4 ± 0.8	1.08 ± 0.59	1.20 ± 0.21	0.97 ± 0.23
CoH^+	1.5 ± 0.4	0.35 ± 0.18	5.83 ± 0.25	4.59 ± 0.23
$CoCH_2^+$	1.6 ± 0.4	0.17 ± 0.13	7.42 ± 0.30	5.95 ± 0.23
		$CoC_2H_4^+ + D_2$		
CoH^+	1.5 ± 0.5[b]	1.12 ± 0.28	4.30 ± 0.30	4.3 ± 0.2
CoD^+	1.5 ± 0.5[b]	0.15 ± 0.08	3.91 ± 0.21	4.3 ± 0.2
$CoCH_2D^+$	3.0 ± 1.1	0.09 ± 0.08	2.65 ± 0.60	2.19 ± 0.22
$CoC_2H_4D^+$	1.5 ± 0.5[b]	1.67 ± 0.56	3.28 ± 0.13	
		$CoCH_2^+ + CH_4$		
Co^+	2.4 ± 0.3	0.14 ± 0.03	0.28 ± 0.10	-0.75 ± 0.06
CoH^+	2.0 ± 0.6	0.18 ± 0.14	2.70 ± 0.40	1.58 ± 0.08
$CoCH_3^+$	2.9 ± 0.6	0.11 ± 0.07	1.11 ± 0.22	0.96 ± 0.07
$CoC_2H_2^+$	1.3 ± 0.3	0.02 ± 0.01	2.57 ± 0.27	1.23 ± 0.06
$CoC_2H_4^+$	1.5 ± 0.2	0.007 ± 0.001	0.50 ± 0.20	-1.23 ± 0.23
		$CoCH_2^+ + CD_4$		
Co^+	2.4 ± 0.1	0.11 ± 0.01	0.34 ± 0.10	-0.75 ± 0.06
CoH^+	2.0 ± 0.9	0.04 ± 0.03	2.73 ± 0.53	1.58 ± 0.08
CoD^+	2.4 ± 0.5	0.10 ± 0.06	2.78 ± 0.32	1.58 ± 0.08
$CoCH_2D^+$	2.9 ± 1.6	0.06 ± 0.04	1.11 ± 0.27	0.96 ± 0.07
$CoCD_3^+$	3.1 ± 0.7	0.08 ± 0.05	1.22 ± 0.21	0.96 ± 0.07
$CoCD_4^+$	2.8 ± 0.6	0.03 ± 0.02	2.50 ± 0.33	2.36 ± 0.08

[a] Calculated using data in Tables 2 and 3 for perprotio species. [b] Analysis was performed by holding n constant over a reasonable range of values.

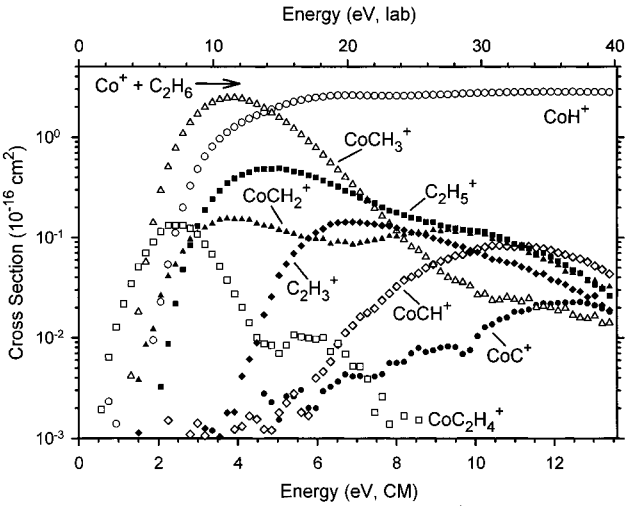

Figure 1. Cross sections for the reaction of Co^+ with ethane as a function of relative kinetic energy (lower x-axis) and laboratory energy (upper x-axis).

the $CoCH_2^+$ product ion from the much more intense $CoCH_3^+$ product. Observation of the $C_2H_3^+$, $CoCH^+$, and CoC^+ product ions, which have even smaller intensities, is reported here for the first time. In the present study, the sensitivity is one to two orders of magnitude better than that of GFA and two to three orders of magnitude better than AB largely because of a much more intense reactant ion beam.

The energetic behavior of the various cross sections is straightforward to understand. Products that obviously involve C−H bond activation will be discussed first. The $CoC_2H_4^+$ product has the lowest threshold among all products observed. We measure a value of 0.32 ± 0.12 eV, Table 4, consistent with the observations and estimate of GFA. This cross section reaches a maximum at an energy consistent with the thresholds for several higher energy products, notably CoH^+ and $C_2H_5^+$. Although formation of $Co^+ + C_2H_4 + H_2$ can begin at about 1.34 eV, no noticeable influence of this decomposition pathway is evident. Rather, as pointed out previously,[4] the decline in the $CoC_2H_4^+$ cross section is most plausibly due to competition with these other reaction channels, indicating that they share a common intermediate. The second feature in the $Co^+(C_2H_4)$ cross section is likely to be the result of $CoC_2H_4^+ + 2H$ formation, which can begin at 4.00 ± 0.22 eV. Although we observe no $CoC_2H_5^+$ product ion that would serve as the precursor for this process, the maximum magnitude for the second feature is only 10^{-18} cm^2, consistent with a $CoC_2H_5^+$ cross section too small to observe readily.

The CoH^+ cross section rises from its thermodynamic threshold and then levels out. Dissociation of this product in the overall process to form $Co^+ + H + C_2H_5$ can begin at $D_0(H-C_2H_5) = 4.31 \pm 0.02$ eV. The failure to observe a decline in the CoH^+ cross section beginning at this energy indicates that the C_2H_5 neutral product carries away significant amounts of energy. The $C_2H_5^+$ product competes directly with CoH^+ as reactions 8 and 9 differ only in location of the charge. As previously discussed by GFA, the relative behavior of these two cross sections indicates that IE(CoH) is slightly less than IE(C_2H_5) = 8.117 ± 0.008 eV.[36] The $C_2H_5^+$ product ion decomposes by dehydrogenation to form $C_2H_3^+$, as shown by the correspondence between the peak in the $C_2H_5^+$ cross section and the threshold for $C_2H_3^+$.

Of the products that involve C−C bond activation, the $CoCH_2^+ + CH_4$ product channel has a cross section that peaks near 4 eV, consistent with the threshold for decomposition in the overall process to $Co^+ + CH_2 + CH_4$, 4.04 ± 0.03 eV. The $CoCH_2^+$ product can also decompose by dehydrogenation to form $CoC^+ + H_2$, accounting for this latter product. The $CoCH_3^+$ cross section rises from its thermodynamic threshold and reaches a maximum near 4 eV. At this point, the product ion can decompose to $Co^+ + CH_3$, a process that can begin at 3.81 ± 0.01 eV = $D_0(CH_3-CH_3)$. $CoCH_3^+$ can also decompose to form $CoCH_2^+ + H$ starting at 5.28 ± 0.06 eV and to form $CoCH^+ + H_2$ starting at 4.05 ± 0.38 eV. The former process accounts for the higher energy feature observed in the $CoCH_2^+$ cross section. The latter process accounts for the $CoCH^+$ product.

As listed in Table 4, most products in this reaction system are measured to have thresholds in agreement with the thermodynamic thresholds calculated from Tables 2 and 3. Exceptions include $CoC_2H_4^+$ and $CoCH_2^+$ which have thresholds higher than the thermodynamic values by 0.80 ± 0.25 and 0.36 ± 0.23 eV, respectively. This suggests that there are barriers to reactions 3 and 5. The CoC^+ and $CoCH^+$ cross sections are difficult to analyze because the cross sections rise slowly and are noisy in the threshold region due to their small intensity. If the E_0 values are held at their thermodynamic values while the other parameters are optimized, then eq 1 can reproduce the cross sections reasonably well.

$CoC_2H_6^+$ + Xe. Figure 2 shows cross sections for the interaction of Xe with $CoC_2H_6^+$ formed by three-body conden-

(36) Berkowitz, J.; Ellison, G. B.; Gutman, D. *J. Phys. Chem.* **1994**, *98*, 2744.

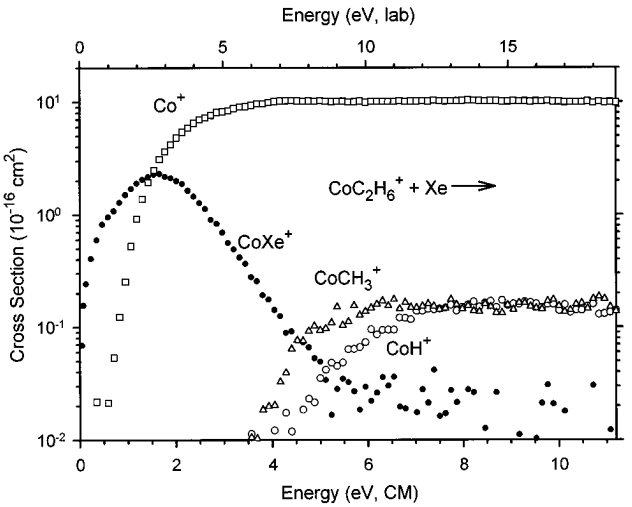

Figure 2. Cross sections for the reaction of $CoC_2H_6^+$ (made by adding ethane to the flow tube) with xenon as a function of relative kinetic energy (lower *x*-axis) and laboratory energy (upper *x*-axis).

sation of ethane and Co^+ in the flow tube. The products observed correspond to reactions 11−14.

$$CoC_2H_6^+ + Xe \rightarrow Co^+ + C_2H_6 + Xe - 1.21 \pm 0.07 \text{ eV} \quad (11)$$

$$\rightarrow CoXe^+ + C_2H_6 - 0.36 \pm 0.10 \text{ eV} \quad (12)$$

$$\rightarrow CoCH_3^+ + CH_3 + Xe - 2.92 \pm 0.08 \quad (13)$$

$$\rightarrow CoH^+ + C_2H_5 + Xe - 3.54 \pm 0.09 \quad (14)$$

It is evident that Co^+, formed by collision-induced dissociation (CID), is the predominant product observed at all energies above about 1.5 eV. Ligand exchange forms $CoXe^+$ and is the predominant process at lower energies. Production of $CoXe^+$ clearly undergoes strong competition with reaction 11 as evidenced by the sharp decline in the $CoXe^+$ cross section once the threshold for CID is exceeded. Both $CoCH_3^+$ and CoH^+ are minor products in this reaction and correspond to the largest products observed in the bimolecular reaction of Co^+ with ethane, Figure 1. It seems likely that other products observed in the bimolecular reaction are also formed, but their intensities are too small to be detected here.

It is important to know the identity of the $CoC_2H_6^+$ structure to determine relevant thermochemistry. Three possible structures are the Co^+(ethane) adduct, cobalt−dimethyl cation, $Co(CH_3)_2^+$, and the hydrido-ethyl−cobalt cation, $H-Co^+-C_2H_5$. To determine the structure of the $CoC_2H_6^+$ complex, we carried out several studies. First is the study shown in Figure 2, CID of $CoC_2H_6^+$ produced by adding ethane to the flow tube. Second, we formed $CoC_2H_6^+$ by the bimolecular reaction of Co^+ with acetone in the flow tube,[37] which might preferentially form $Co(CH_3)_2^+$. CID of this isomer should yield appreciable amounts of $CoCH_3^+ + CH_3$, in analogy with our observations on $Fe(CH_3)_2^+$.[29] Instead, CID results for the $CoC_2H_6^+$ ion formed in this fashion were identical to those in Figure 2. This suggests that only the Co^+(ethane) isomer is being produced, with little or no cobalt dimethyl isomer. This conclusion is in good agreement with recent studies of Carpenter *et al.*[38] Third, to remove as much internal energy from the $CoC_2H_6^+$ species as possible (which might allow isomerization to occur), we produced this ion by using ligand exchange reactions in the flow tube. This was achieved by first adding methane to the flow tube near the Co^+ source and then adding ethane or acetone about 60 cm downstream. In both cases, the CID results on the $CoC_2H_6^+$ species produced were identical to those shown in Figure 2. All these results point to a Co^+(ethane) adduct structure.

Analysis of the Co^+ cross section is straightforward and yields a threshold, Table 4, that agrees with literature values for the Co^+−ethane bond energy, Table 3, as described in more detail below. This confirms our identification of the structure of $CoC_2H_6^+$ as the Co^+−ethane complex. The $CoXe^+$ cross section was difficult to model because of its complicated shape; however, the cross section can be reproduced with eq 1 and the thermodynamic threshold, Table 3. When the cross sections for the $CoCH_3^+$ and CoH^+ products are analyzed over most of the energy range shown, eq 1 yields the optimized parameters given in Table 4. These measured thresholds are higher than their thermodynamic values, although they have the correct relative values. However, these cross sections can also be reproduced nicely with eq 1 and E_0 values equal to the thermodynamic threshold (with a concomitant increase in the *n* parameter). Thus, the apparent shift to higher energies is caused by strong competition with the CID channel, which is favored for both thermodynamic and kinetic reasons. Simple CID should occur through a loose transition state from the Co^+-(C_2H_6) adduct, while C−C and C−H bond activation processes require rearrangement through tight transition states.

$CoC_2H_4^+$ + Xe. Cross sections for the interaction of Xe with $CoC_2H_4^+$ formed by three-body condensation of ethene and Co^+ in the flow tube are shown in Figure 3. The products observed correspond to reactions 15−18.

$$CoC_2H_4^+ + Xe \rightarrow Co^+ + C_2H_4 + Xe - 1.82 \pm 0.22 \text{ eV} \quad (15)$$

$$\rightarrow CoXe^+ + C_2H_4 - 0.97 \pm 0.23 \text{ eV} \quad (16)$$

$$\rightarrow CoCH_2^+ + CH_2 + Xe - 5.95 \pm 0.23 \text{ eV} \quad (17)$$

$$\rightarrow CoH^+ + C_2H_3 + Xe - 4.59 \pm 0.23 \text{ eV} \quad (18)$$

The dominant process is simple CID to form Co^+, reaction 15. Analysis of this cross section yields a threshold, Table 4, that agrees nicely with literature values for the Co^+−ethene bond energy, Table 3. This clearly identifies the structure of the $CoC_2H_4^+$ ion as the Co^+(ethene) complex. The ligand exchange reaction to form $CoXe^+$ competes strongly with CID, as shown by the strong decline in this product once the threshold for CID is exceeded.

The $CoXe^+$ product cross section exhibits a small exothermic feature that is matched by a small endothermic feature at the lowest energies in the Co^+ cross section. These features do not depend on the neutral reactant pressure and are reproducible (observed in every data set taken over a 3-year period). This discounts the possibility that they are due to trace impurities. It seems likely that we have a small amount of unquenched excited states, although drastic changes in the dc discharge conditions and flow gas ratios did not eliminate the low energy features.

(37) Halle, L. F.; Crowe, W. E.; Armentrout, P. B.; Beauchamp, J. L. *Organometallics* **1984**, *3*, 1694.

(38) Carpenter, C. J.; van Koppen, P. A. M.; Bowers, M. T. *J. Am. Chem. Soc.* **1995**, *117*, 10976.

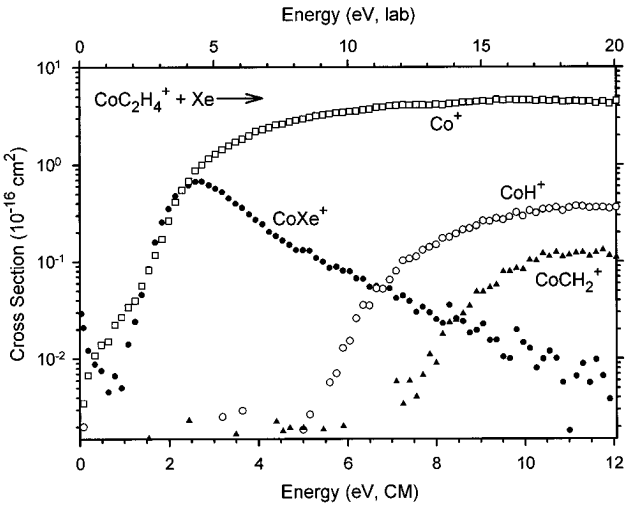

Figure 3. Cross sections for the reaction of $CoC_2H_4^+$ (made by adding ethene to the flow tube) with xenon as a function of relative kinetic energy (lower *x*-axis) and laboratory energy (upper *x*-axis).

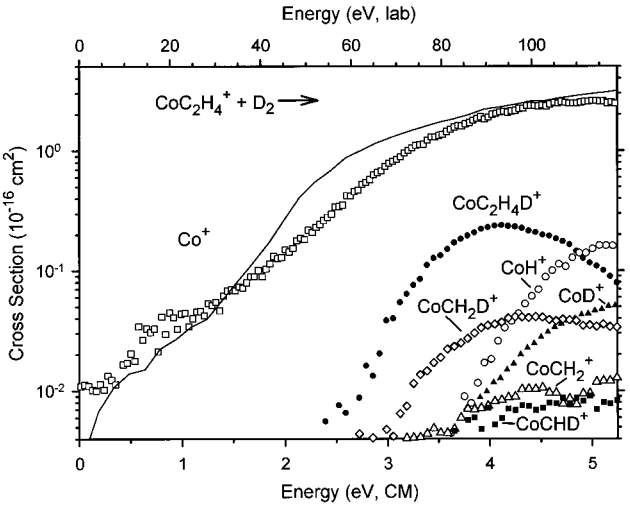

Figure 4. Cross sections for the reaction of $CoC_2H_4^+$ with D_2 as a function of relative kinetic energy (lower *x*-axis) and laboratory energy (upper *x*-axis). The line is the Co^+ cross section taken from the reaction of $CoC_2H_4^+ + Xe$, Figure 3.

A similar low-energy tail was also observed in our study of the $Co^+(C_3H_6) + Xe$ system, where this complex was made by adding propene, cyclopropane, or cyclobutanone to the flow tube.[10] For each method of preparation, the low-energy tail in the $Co^+(C_3H_6)$ CID cross section had a similar magnitude and threshold to that observed here. Analysis of the low-energy tail on the Co^+ cross section with eq 1 yields a threshold of 0.4 ± 0.1 eV when *n* is held to a value of 1. This indicates an excitation energy of about 1.5 eV, which could indicate involvement of the a^1D state of Co^+ (1.444 eV higher than the a^3F ground state)[39] or perhaps the a^5F state (which should bind ethene much more weakly than the a^3F state because the 4s orbital is occupied). The presence of these low-energy features complicates the analysis of the Co^+ and $CoXe^+$ cross sections somewhat. The cross sections were modeled both by ignoring the low-energy features and by modeling them and subtracting the model from the data before further analysis. The uncertainties listed in Table 4 include both types of analyses, although the differences between the two modeling methods are small because of the small size of the low-energy features.

(39) Sugar, J.; Corliss, C. J. *J. Phys. Chem. Ref. Data, Suppl.* **1985**, *14*, Supp. 2.

The two minor product ions observed in Figure 3, CoH^+ and $CoCH_2^+$, correspond to the primary products observed in the bimolecular reaction of Co^+ and ethene.[8] When analyzed over an extended energy range, the thresholds measured for these products are larger than their thermodynamic values, Table 4. We can also reproduce these cross sections with eq 1 and the thermodynamic thresholds, such that we again attribute the behavior to competition with the thermodynamically and kinetically favored CID process. The apparent shifts observed for reactions 17 and 18 in the $CoC_2H_4^+$ system are larger than those of the comparable processes, reactions 13 and 14, in the $CoC_2H_6^+$ system. This is consistent with higher thermodynamic thresholds in the former system.

$CoC_2H_4^+ + D_2$ (H_2). The dominant product formed in the reaction of $CoC_2H_4^+$ with D_2 is Co^+, with a cross section shown in Figure 4. This cross section can be explained by processes 19a and 19b. Other minor products observed correspond to reactions 20−23.

$$CoC_2H_4^+ + D_2 \rightarrow Co^+ + C_2H_4D_2 - 0.48 \pm 0.22 \text{ eV} \quad (19a)$$

$$\rightarrow Co^+ + C_2H_4 + D_2 - 1.82 \pm 0.22 \text{ eV} \quad (19b)$$

$$\rightarrow CoC_2H_4D^+ + D \quad (20)$$

$$\rightarrow CoCH_2D^+ + CH_2D - 2.19 \pm 0.22 \text{ eV} \quad (21)$$

$$\rightarrow CoCHD^+ + CH_3D - 1.23 \pm 0.23 \text{ eV} \quad (22a)$$

$$\rightarrow CoCH_2^+ + CH_2D_2 - 1.23 \pm 0.23 \text{ eV} \quad (22b)$$

$$\rightarrow CoH^+ + C_2H_3D + D - 4.3 \pm 0.2 \text{ eV} \quad (23a)$$

$$\rightarrow CoD^+ + C_2H_4 + D - 4.3 \pm 0.2 \text{ eV} \quad (23b)$$

Reaction of $Co^+(C_2H_4)$ with H_2 was also performed. The only product observed was Co^+, process 19. Given the small size of the cross sections in all cases but the Co^+ product, useful results for the minor products could not be obtained. Because of the large laboratory to center-of-mass energy scale conversion, these minor products are not formed until over 100 eV (lab) in the H_2 system and therefore are not collected efficiently when the quadrupole mass resolution is sufficiently high to distinguish them.

The cross section for Co^+ clearly has two features. Below 1.5 eV, it rises from an apparent threshold near 0.3 eV and reaches a magnitude of about 0.04 Å^2. It is tempting to attribute this part of the cross section to reaction 19a, the formation of ethane. However, the magnitude and shape of this part of the cross section are comparable to the low-energy feature observed and described in the $CoC_2H_4^+ + Xe$ system, Figure 3. Further, on the basis of the threshold observed for reaction 19, we expect reaction 19a to have a threshold of 0.80 ± 0.25 eV (=0.48 eV endothermicity + 0.32 eV barrier), while analysis of the cross section here yields a threshold of about 0.4 ± 0.2 eV. Thus, it appears that most of the low-energy feature in the Co^+ cross section can be attributed to the same metastable $CoC_2H_4^+$ species observed in the reaction with Xe, where no ethane can possibly be formed. We conclude that there is no *conclusive* evidence for process 19a although our sensitivity to this process

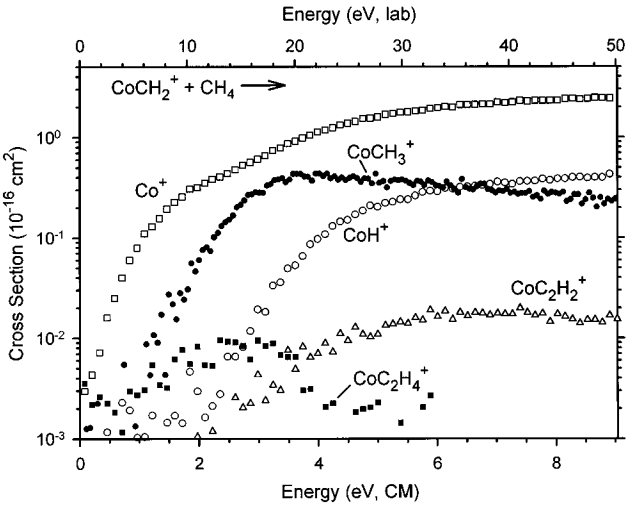

Figure 5. Cross sections for the reaction of $CoCH_2^+$ with CH_4 as a function of relative kinetic energy (lower *x*-axis) and laboratory energy (upper *x*-axis).

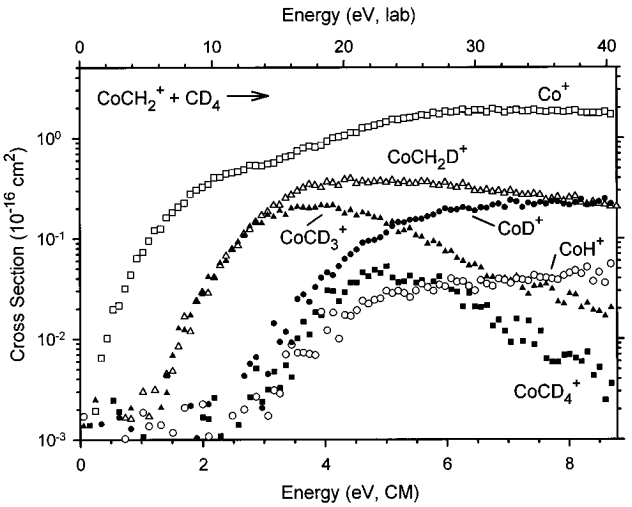

Figure 6. Cross sections for the reaction of $CoCH_2^+$ with CD_4 as a function of relative kinetic energy (lower *x*-axis) and laboratory energy (upper *x*-axis).

is mitigated by the interference of the metastable CID process. Beginning at about 1.5 eV, the Co^+ cross section increases more rapidly, a result that can be attributed to CID of the ground state $CoC_2H_4^+$ complex, process 19b. The apparent threshold observed differs from the 1.82-eV endothermicity because of the kinetic energy distributions of the reactants. The Co^+ cross section from reaction 19 rises more slowly than that from reaction 15, a common observation for a light target gas.[28,40]

There is some ambiguity about the identification of the $CoCH_2^+$, $CoCHD^+$, and $CoCH_2D^+$ products as they have the same masses as $CoCD^+$, $CoCH_3^+$, and $CoCD_2^+$, respectively. All three cross sections rise from apparent thresholds of about 3 eV, thereby offering no clear differentiation among products. Such a threshold is consistent with Co^+−methyl products and also demonstrates that any $CoCH_xD_{2-x}^+$ products are accompanied by $CH_{4-x}D_x$ neutral products. Such a threshold also rules out a $CoCD^+$ product because its thermodynamic threshold is about 4.5 eV, although such a product could be formed at higher energies. Thus, there is little ambiguity regarding the identity of the $CoCH_2^+$ cross section. The $CoCH_2D^+/CoCD_2^+$ product ion has the largest cross section of these product ions. We can think of no rational mechanism that would preferentially form $CoCD_2^+$ in much greater abundance than $CoCH_2^+$, hence this cross section is attributed to $CoCH_2D^+$. The most problematic of these products is the $CoCHD^+/CoCH_3^+$ channel, in part because the mass resolution conditions needed to obtain efficient collection of these products also allow an estimated 10 ± 10% overlap with the more intense $CoCH_2D^+$ product ion. The $CoCHD^+/CoCH_3^+$ cross section is shown uncorrected for this overlap, but such a correction leads to a cross section that is half the magnitude shown or possibly completely gone. We attribute this cross section primarily to the $CoCHD^+$ product, largely because formation of $CoCH_3^+ + CHD_2$ implies that $CoCHD_2^+ + CH_3$ should also be formed with a comparable yield. This product was not observed, although because of the small size of these cross sections, such a failure is not definitive. Other mechanistic reasons for the $CoCHD^+$ assignment are discussed below.

The cross sections for formation of CoH^+ and CoD^+ rise from similar thresholds between 4 and 4.5 eV. The CoH^+ cross section has been corrected for overlap with the much more intense Co^+ product, such that the uncertainty in this cross section near threshold is larger than that for most products. The neutral products accompanying these product ions could be $C_2H_3D_2$ and C_2H_4D, respectively, or $C_2H_3D + D$ and $C_2H_4 + D$, respectively. The former reactions have thresholds of about 2.8 ± 0.2 eV, while the latter can begin at about 4.3 ± 0.2 eV. The results are more consistent with the latter process, although the possibility of barriers or delayed thresholds due to competition cannot be completely eliminated.

$CoCH_2^+ + CH_4$ (CD_4). Results for the reaction $CoCH_2^+ + CH_4$ are shown in Figure 5. Products correspond to reactions 24−29.

$$CoCH_2^+ + CH_4 \rightarrow Co^+ + C_2H_6 + 0.75 \pm 0.06 \text{ eV} \quad (24a)$$

$$\rightarrow Co^+ + CH_2 + CH_4 - 3.29 \pm 0.05 \text{ eV} \quad (24b)$$

$$\rightarrow CoH^+ + C_2H_5 - 1.58 \pm 0.08 \text{ eV} \quad (25)$$

$$\rightarrow CoCH_3^+ + CH_3 - 0.96 \pm 0.07 \text{ eV} \quad (26)$$

$$\rightarrow CoCH_4^+ + CH_2 - 2.36 \pm 0.08 \text{ eV} \quad (27)$$

$$\rightarrow CoC_2H_2^+ + 2H_2 - 1.23 \pm 0.06 \text{ eV} \quad (28)$$

$$\rightarrow CoC_2H_4^+ + H_2 + 1.23 \pm 0.23 \text{ eV} \quad (29)$$

Additional information regarding this reaction system can be obtained by performing this experiment using deuterated methane, CD_4, as shown in Figure 6. The results are in good agreement with those of Figure 5.

Reactions 24a and 29 are exothermic but the Co^+ and $CoC_2H_4^+$ cross sections exhibit clear thresholds, indicating reaction barriers to both processes. Co^+ is the dominant product over the energy range studied. Above about 3 eV, this cross section increases more rapidly, consistent with the onset of reaction 24b, the simple CID process. Analysis of the Co^+ cross section with eq 1 yields a threshold of 0.28 ± 0.10 eV for the CH_4 reaction and 0.34 ± 0.10 for the CD_4 reaction, Table 4. The $CoC_2H_4^+$ cross section rises from a threshold at about the

(40) Aristov, N.; Armentrout, P. B. *J. Phys. Chem.* **1986**, *90*, 5135. Hales, D. A.; Armentrout, P. B. *J. Cluster Sci.* **1990**, *1*, 127.

same energy, between 0.3 and 0.7 eV, Table 4, and declines when the CoH^+ and $CoC_2H_2^+$ cross sections begin, indicating competition between these product channels. In the CD_4 system, isotope scrambling is observed for the $CoC_2H_x^+$ products. Both $CoC_2H_2D_2^+$ and $CoC_2HD_3^+$ are observed and have cross sections ≤ 0.01 Å^2. Because of their small intensities, we were not able to unambiguously differentiate individual cross sections for these products and those for the $CoC_2H_2^+$ analogues where $CoC_2D_2^+$, CoC_2HD^+, and $CoC_2H_2^+$ were formed with cross section ≤ 0.01 Å^2. Analysis of the $CoC_2H_2^+$ cross section in the CH_4 system provides a threshold of 2.57 ± 0.27 eV, Table 4, higher than its thermodynamic value of 1.23 eV, although this cross section is sufficiently small that the threshold analysis is not definitive. This delayed threshold is most likely due to strong competition with the CoH^+ and $CoC_2H_4^+$ channels.

The threshold measured for CoH^+ is consistent with that calculated for the formation of C_2H_4 + H as neutral products, Table 4, but could also correspond to formation of CoH^+ + C_2H_5 with a threshold pushed to higher energies by competition. The Co−hydride ion channels in the CD_4 system show both CoH^+ and CoD^+. These cross sections rise from similar thresholds with similar energy dependencies. CoD^+ is favored over CoH^+, such that CoD^+ comprises $80 \pm 5\%$ of the sum of the CoD^+ and CoH^+ cross sections.

$CoCH_3^+$ is also an abundant product and begins at an apparent threshold near its thermodynamic value. The cobalt−methyl ion channels formed in the CD_4 system exhibit two products, $CoCD_3^+$ and $CoCH_2D^+$. These products rise from the same threshold with identical intensities, but the former declines above about 3.5 eV while the latter is relatively constant over the same energy range. The decline must be due to dissociation of this product to $Co^+ + CD_3$, which can begin at 3.06 ± 0.08 eV. The $CoCH_2D^+$ product could also begin to decompose at this energy. This difference in behavior is discussed below.

$CoCH_4^+$ was observed in the CH_4 system, but is not shown in Figure 5 because the results are noisy due to the high-resolution conditions required to separate this product from the more intense neighboring $CoCH_3^+$ product ion. The $CoCD_4^+$ product in the CD_4 system rises from a threshold consistent with its thermodynamic threshold. The failure to observe any H/D scrambling shows that this product is formed in a simple ligand exchange process.

Thermochemistry

$Co^+-C_2H_6$. From the CID reaction of $CoC_2H_6^+ + Xe$, we measure a 0 K threshold of 1.04 ± 0.05 eV for $CoC_2H_6^+$ to dissociate into Co^+ and ethane, Table 3. This threshold should be a direct measure of the $Co^+-C_2H_6$ BDE, because this is a simple bond fission and the interaction of Co^+ with ethane should be attractive at long range. This BDE of 1.04 ± 0.05 eV is somewhat lower than the experimental result from Kemper *et al.*[13] of 1.21 ± 0.07 eV, but agrees well with a theoretical D_0 value calculated by Perry *et al.*[25] of 1.06 eV. These authors then estimate a correction for their calculated bond energy of 0.09 ± 0.09 eV, such that their best estimated D_0 value is 1.14 $\pm$ 0.09 eV, in good agreement with both experimental values. Holthausen and Koch (HK)[18] obtain $D_e(Co^+-C_2H_6) = 1.26$ eV, which can be corrected to $D_0(Co^+-C_2H_6) = 1.23$ eV using the zero point energy correction estimated by Perry *et al.* for this BDE.[25]

The agreement between these various measurements is acceptable considering the weakness of the bonds being probed. Nevertheless, it is worth exploring possibilities for the discrepancy. It is conceivable that our $Co^+-C_2H_6$ BDE is smaller than that of Kemper *et al.* because our ions are not completely thermalized. However, the difference of 0.17 ± 0.09 eV corresponds to a temperature of about 2000 ± 1000 K, and it is unlikely that our ions have internal excitation this high. It is conceivable that our ions have a small population of electronically excited states (as observed for $CoC_2H_4^+$), but we expect that these should be evident in the Co^+ and $CoXe^+$ cross sections. Careful inspection of our data, Figure 2, shows no low-energy tails for either of these products.

$Co^+-C_2H_4$. From the CID reaction of $CoC_2H_4^+ + Xe$, Figure 3, we measure a 0 K threshold of 1.86 ± 0.07 eV for the dissociation of $CoC_2H_4^+$ into $Co^+ + C_2H_4$, Table 3. This value corresponds to the Co^+-ethene BDE and is in good agreement with a lower limit measured from the reaction of $Co^+ + c\text{-}C_3H_6$, $D_{298}(Co^+-C_2H_4) > 1.73 \pm 0.20$ eV.[41] It also agrees with a value of 1.82 ± 0.22 eV determined by van Koppen *et al.*[42] Three theoretical values have been calculated. Sodupe *et al.*[22] used the MCPF method with geometries determined at the Hartree−Fock level to calculate $D_e(Co^+-C_2H_4) = 1.58$ eV. Perry used a higher level of theory to determine the geometries and calculated $D_e(Co^+-C_2H_4) = 1.95$ eV.[17] The density functional calculation of HK obtains $D_e = 2.21$ eV.[18] On the basis of the vibrational frequencies listed in Table 1, we estimate that the zero point energy correction is 0.07 ± 0.02 eV. Thus, the three theoretical values correspond to $D_0(Co^+-C_2H_4)$ values of 1.51, 1.88, and 2.14 eV, respectively, in reasonable agreement with our experimental value of 1.86 ± 0.07 eV.

The BDE for $Co^+-C_2H_4$, 1.86 ± 0.07 eV, is stronger than the BDE for Co^+-ethane, 1.04 ± 0.05 eV. The same trend is also observed in the Co^+-propene bond, 1.87 ± 0.07 eV,[10] and the Co^+-propane bond, 1.34 ± 0.06 eV.[43] This seems consistent with the idea that the π electrons of alkenes make them much better electron donors than the saturated alkanes. Perry[17] suggests that the Co^+-ethene bond is predominantly electrostatic and leads to π-complexes following the Dewar−Chatt−Duncanson bonding model.[44]

$CoC_2H_4D^+$. The $CoC_2H_4D^+$ species formed in reaction 20 can conceivably have a cobalt−ethyl, $Co^+-C_2H_4D$, or $DCo^+(C_2H_4)$ structure. Insight into which structure is being formed may be found by looking at the Co^+-hydride channels (CoH^+ and CoD^+) in reactions 23a and 23b. As mentioned above, the thresholds of these channels indicate that the likely neutrals formed are C_2H_3D + D and C_2H_4 + D, respectively. A mechanism for the latter reaction is decomposition of $CoC_2H_4D^+$ to $CoD^+ + C_2H_4$. This dissociation pathway is thermodynamically favored by 0.15 ± 0.09 eV over the alternate pathway to $Co^+(C_2H_4)$ + D, Table 3. The observation of appreciable CoH^+ formation in Figure 4 demonstrates that the $CoC_2H_4D^+$ ion scrambles the H and D atoms. An obvious mechanism is the rearrangement of $DCo^+(C_2H_4)$ to $Co^+-CH_2CH_2D$ and back to $HCo^+(C_2H_3D)$ by sequential β-H or β-D transfers. Complete scrambling between the H and D atoms would give a CoH^+ to CoD^+ ratio of 4:1 or 80% CoH^+. Incomplete scrambling would lower this percentage. This is consistent with our results in which CoH^+ is found to comprise $75 \pm 5\%$ of the sum of the CoH^+ and CoD^+ cross sections. In contrast, complete scrambling in a $(D)_2Co^+(C_2H_4)$ intermediate would lead to 66% CoH^+ (and incomplete scrambling to a lower percentage), in poorer agreement with experiment.

(41) Fisher, E. R.; Armentrout, P. B. *J. Phys. Chem.*, **1990**, *94*, 1674.
(42) van Koppen, P. A. M.; Bowers, M. T.; Beauchamp, J. L.; Dearden, D. V. *ACS Symp. Ser.* **1990**, *428*, 34.
(43) Haynes, C. L.; Fisher, E. R.; Armentrout, P. B. Work in progress.
(44) Crabtree, R. H. In *The Organometallic Chemistry of the Transition Metals*; Wiley: New York, 1988; Chapter 5. Lukehart, C. M. *Fundamental Transition Metal Organometallic Chemistry*; Brooks/Cole: Monterey, 1985.

Another potential way of ascertaining which structure is formed at threshold is to consider the thermodynamics. The threshold measured for reaction 20 leads to $D_0[D-Co^+(C_2H_4)] = 1.28 \pm 0.13$ eV, substantially weaker than $D_0(Co^+-D) = 2.01 \pm 0.06$ eV, Table 3. Alternatively, we can use this threshold to determine $D_0(DCo^+-C_2H_4) = 1.13 \pm 0.16$ eV, much weaker than $D_0(Co^+-C_2H_4) = 1.86 \pm 0.07$ eV. It is reasonable that these BDEs decrease because the Co^+-D bond utilizes the 4s orbital on the metal, while strong bonding of C_2H_4 to Co^+ relies on having an empty 4s orbital. A useful comparison is therefore the diabatic BDE for $Fe^+(^6D,4s^13d^6)$ to C_2H_4. This cannot be measured directly because the ground state of $Fe^+(C_2H_4)$ is a quartet.[22] Sodupe *et al.*[22] calculate that the sextet state BDE is 0.23 eV weaker than the adiabatic BDE for the quartet ground state which has been measured as 1.50 ± 0.06 eV.[33] Thus, an estimate for the sextet BDE is 1.27 ± 0.06 eV. Therefore, the BDE of ethene to CoD^+ is comparable to that for $Fe^+(^6D)$, indicating that the threshold is consistent with formation of the $DCo^+(C_2H_4)$ isomer. Alternatively, we could assign this threshold to production of the cobalt−ethyl structure, which leads to a $Co^+-C_2H_4D$ BDE of 1.59 ± 0.15 eV.[45] Experimentally, the $Co^+-C_2H_5$ BDE has been measured in a study of the reaction of Co^+ + propane where the measured threshold for production of $CoC_2H_5^+$ yields a lower limit to the $Co^+-C_2H_5$ BDE of $>1.76 \pm 0.09$ eV. Later it was suggested[33] that the BDE should equal 2.00 ± 0.11 eV based on a comparison of the relative thresholds for production of $CoCH_3^+ + C_2H_5$ and $CoC_2H_5^+ + CH_3$ in this system. The latter bond energy is probably correct given theoretical results that suggest that the Co^+-CH_3 BDE (2.10 ± 0.04 eV, Table 3) is higher than $Co^+-C_2H_5$ BDE by 0.07 eV[17] and lower by 0.30 eV.[18] Thus, the threshold obtained here is inconsistent with formation of the cobalt−ethyl ion structure.

Finally, we note that no $CoC_2H_5^+$ species is formed in any of the other reaction systems studied here. Based on the mechanism of Scheme 1, we might have expected to see $Co^+-C_2H_5$ formed in the $Co^+ + C_2H_6$ system by decomposition of intermediate **2**, although this product is disfavored compared to CoH^+ on the basis of angular momentum arguments.[46] This suggests that a $DCo^+(C_2H_4)$ product is probably formed in a direct reaction between $Co^+(C_2H_4)$ and D_2, although this species can rapidly equilibrate with the Co^+−ethyl structure as demonstrated by the isotope scrambling results in the cobalt−hydride ion channels.

$CoCH_2D^+$. The $CoCH_2D^+$ species formed in reactions 21b and 26 can conceivably have a cobalt−methyl, Co^+-CH_2D, or $DCoCH_2^+$ structure. Simple bond additivity indicates that the $DCoCH_2^+$ isomer is 1.5 ± 0.3 eV higher in energy than the Co^+-CH_2D isomer, and an estimate that considers promotion energies finds a similar result. In the reaction of $Co^+(C_2H_4) + D_2$, reaction 21b, the $CoCH_2D^+$ cross section rises from a threshold consistent with the production of $Co^+-CH_2D + CH_2D$. This makes sense if D_2 adds across the C=C bond (although there is no implication that this is a concerted addition).

In the reaction of $CoCH_2^+ + CD_4$, process 26, formation of $CoCH_2D^+$ and $CoCD_3^+$ rises from thresholds indicating a Co^+−methyl structure. At higher energies, the $CoCD_3^+$ cross section drops off rapidly because this product dissociates to $Co^+ + CD_3$. In contrast, the $CoCH_2D^+$ cross section remains constant. It is possible that this difference is because the CD_3 neutral carries away more of the excess internal energy than CH_2D, which is plausible because CD_3 has a higher mass and density of vibrational states than CH_2D. However, such a dramatic difference in behavior is surprising. Another possibility is that there is a direct pathway for formation of $CoCH_2D^+$. Such a pathway could be a direct D atom abstraction from CD_4 to form $DCoCH_2^+$, the higher energy isomer. If the $CoCD_3^+$ cross section is subtracted from the $CoCH_2D^+$ cross section, analysis of the remaining cross section yields a threshold of 2.94 ± 0.18 eV. This is 1.83 ± 0.32 eV above the primary threshold, consistent with the formation of the $DCoCH_2^+$ isomer at these higher energies.

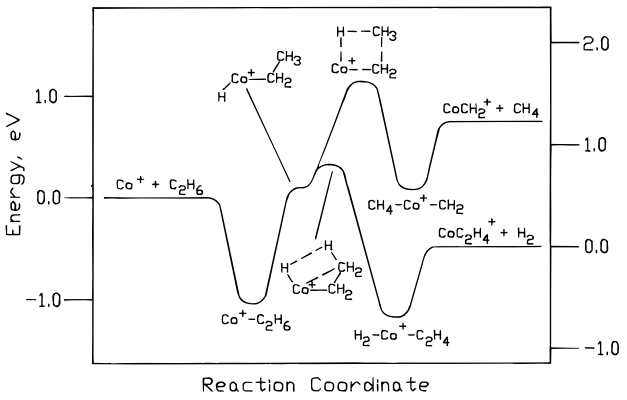

Figure 7. Potential energy surface for C−H bond activation in the interaction of $Co^+ + C_2H_6$.

Discussion

C−H Bond Activation of Ethane. The threshold measured for reaction 3, 0.32 ± 0.12 eV, is a direct determination of the barrier height for the dehydrogenation reaction of $Co^+ + C_2H_6$. Combined with the information from calculations by Perry[17] and Holthausen and Koch (HK),[18] we can now construct a quantitative PES for the dehydrogenation reaction of ethane by Co^+. Both theoretical studies calculate that the limiting transition state (TS) for dehydrogenation of ethane by Co^+ corresponds to a structure similar to intermediate **2**, $H-Co^+-C_2H_5$, where the Co−H and C−C bonds are eclipsed, Figure 7. The energy of this TS is calculated as 0.87 eV by HK and 0.46 eV by Perry, who then estimates a value of 0.22 eV.[17] Either of Perry's values is in good agreement with our measured barrier. The lowest energy isomer of **2** has a staggered configuration and is calculated to lie 0.09 eV below the $Co^+ + C_2H_6$ asymptote by HK and 0.29 eV above (estimated as 0.04 eV above) by Perry. The $(H_2)Co^+(C_2H_4)$ intermediate is calculated to lie 0.74 eV (estimated as 0.70 eV) below the $Co^+(C_2H_4) + H_2$ asymptote by Perry[17] and 0.69 eV by HK.[18] Overall, the theoretical work can be combined with experimentally determined values for $D_0(Co^+-C_2H_6)$, $D_0(Co^+-C_2H_4)$, and the barrier height to give the detailed potential energy surface for the dehydrogenation of ethane shown in Figure 7.

Given this potential energy surface, we can now rationalize our observations regarding the dehydrogenation of ethane and its reverse. In the forward direction, the exothermic dehydrogenation reaction of $Co^+ + C_2H_6$ to form $Co^+(C_2H_4) + H_2$ has a barrier. This barrier lies below the threshold energies of all other reaction channels such that dehydrogenation is the only process observed at low energies, Figure 1. The $Co^+(C_2H_4)$ product cross section does not decrease until the $H-Co^+-C_2H_5$ intermediate **2** formed can decompose to $CoH^+ + C_2H_5$ or $C_2H_5^+ + CoH$. As either of these decompositions has a loose transition state, CoH^+ formation (the thermodynamically favored of the two) dominates the product spectrum once it is energetically accessible. This depletes **2** such that the $Co^+(C_2H_4)$ product cross section decreases.

(45) This value uses an estimated C_2H_4-D BDE that is 0.04 eV greater than the C_2H_4-H BDE, Table 2.

(46) Aristov, N.; Armentrout, P. B. *J. Phys. Chem.* **1987**, *91*, 6178.

In the reverse direction, reaction of $Co^+(C_2H_4)$ with H_2 (D_2), there is now a significant barrier to reaction of 0.84 ± 0.14 eV, a point discussed in some detail by Perry.[17] Therefore, the formation of all products except for Co^+ is inefficient, Figure 4. Indeed, the dominant ionic products observed, Co^+ and $CoC_2H_4D^+$, can be explained without oxidative addition of the D_2 molecule at all. As discussed above, Co^+ is generated primarily in the simple CID process with no clear evidence for concomitant formation of ethane (although an inefficient production of ethane cannot be ruled out). As discussed in the previous section, the $CoC_2H_4D^+$ product is likely to be $DCo^+(C_2H_4)$ formed in a direct process. Even the minor CoH^+ and CoD^+ channels are likely formed by decomposition of the $DCo^+(C_2H_4)$ product.

Compared with the reactivity of the bare Co^+ ion, $Co^+(C_2H_4)$ is less reactive with H_2 because the σ donation from ethene to Co^+ increases the 4s acceptor orbital occupancy on Co^+, while the π back-bonding from Co^+ to ethene removes π electrons from the metal. As discussed in detail elsewhere,[2,47] efficient H_2 activation occurs when the metal center has an empty σ acceptor orbital and occupied π orbitals. Thus, ligation by C_2H_4 moves electrons on the cobalt ion center in ways that are counterproductive for σ bond activation. Perry[17] offers an alternative, but related way of explaining this observation. He notes that in order to efficiently activate H_2 and form two strong Co−H bonds, the Co^+ center must utilize 4s−3d hybridization. When this occurs, however, the 4s orbital has a repulsive interaction with the ethene ligand, thereby destabilizing the H_2-$Co^+(C_2H_4)$ dihydride complex. The relationship between these views is that addition of the $\sigma(H_2)$ bonds to the empty 4s orbital of $Co^+(^3F,3d^8)$ and π back-donation of $3d\pi(Co^+)$ orbitals to $\sigma^*(H_2)$ leads smoothly to the 4s−3d hybridization in a CoH_2^+ intermediate.

C−C Bond Activation of Ethane. C−C bond activation also occurs in the reaction of Co^+ with ethane. The lowest energy C−C bond activation process is the production of $CoCH_2^+ + CH_4$, reaction 5, for which we measure a threshold in excess of the endothermicity by 0.36 ± 0.23 eV, Table 4. The reverse reaction $CoCH_2^+ + CH_4$ to form $Co^+ + C_2H_6$ allows us to measure this barrier more directly, as reaction 24 is the major process at all energies. We observe a threshold for this reaction of 0.28 ± 0.10 eV. The weighted average[48] of these two numbers, 0.29 ± 0.09 eV, is our best determination of the barrier height for demethanation of ethane by Co^+. In the $CoCH_2^+ + CD_4$ system, we measure a barrier of 0.34 ± 0.10 eV, in agreement with this average and also consistent with a small difference due to zero point energy effects.

Insight into the mechanism for C−C bond activation by Co^+ is provided by the reverse of the demethanation reaction, e.g. $CoCH_2^+ + CH_4$ (CD_4). Co^+ is the dominant product observed, with obvious features corresponding to ethane formation and simple CID, Figures 5 and 6. Formation of $CoCH_3^+$ and CoH^+ channels is fairly efficient, contrasting with the inefficient σ bond activation observed in the $Co^+(C_2H_4) + H_2$ system. One reason for this difference is the much lower barrier in the former system (0.29 ± 0.09 eV) versus that in the latter system (0.84 ± 0.14 eV). From the reaction of $CoCH_2^+ + CD_4$, we observe equal amounts of $CoCD_3^+$ and $CoCH_2D^+$ at energies <3 eV. This clearly implicates a $(CH_2D)Co^+(CD_3)$ intermediate analogous to **1**. It also demonstrates that no scrambling of the hydrogen isotopes occurs because a statistical distribution of isotopes would yield a $CoCHD_2^+$ product three times more intense than the $CoCH_2D^+$ and $CoCD_3^+$ products. Bond additivity can be used to estimate that the energy of **1** is 0.40 eV below the $Co^+ + C_2H_6$ asymptote. More sophisticated estimates that consider promotion energies find that the promotion energies for the first and second covalent bonds to Co^+ are nearly equal, such that simple bond additivity should be approximately correct. Calculations concerning the $Co(CH_3)_2^+$ species find D_e values for breaking both Co−C bonds of 3.65,[23] 3.80,[24] and 4.42[18] eV, with an average of 3.96 ± 0.41 eV. On the basis of vibrational frequencies taken from these calculations, the frequencies of the CH_3 radical, and estimates for the remaining low frequency modes of the dimethyl intermediate (assumed to equal 300 ± 300 cm^{-1}), we estimate that the average D_0 value is 4.1 ± 0.4 eV. Given $D_0(CH_3-CH_3) =$ 3.812 eV, Table 2, this puts the dimethyl intermediate about 0.3 ± 0.4 eV below the $Co^+ + C_2H_6$ asymptote, in reasonable agreement with the bond additivity assumption.

There is some controversy regarding the TS between the $Co^+ + C_2H_6$ reactants and the cobalt dimethyl ion intermediate **1**. HK calculate that this TS lies 0.26 eV below the reactants,[18] while Perry suggests that there is a large barrier based on the work of Low and Goddard,[49] although he does not specify a value for the barrier height.[17] In previous work on the $Fe^+ + C_3H_8$ system,[30] the C−C bond activation barrier was found to lie above the C−H bond activation barrier by about 0.5 ± 0.2 eV.[50] In an analysis of the activation of C−C bonds in acetone by Co^+, Carpenter *et al.* suggest that the barrier for C−C bond activation exceeds that for C−H bond activation by 0.26 ± 0.22 eV.[38] In contrast, the calculations of HK indicate that the difference is 0.22 eV with the TS for C−C bond activation lying below that for C−H bond activation. These values have a range of 0.3 ± 0.4 eV, a conservative estimate of the value in the present system. The energy of the C−H bond activation transition state in the present system (the staggered geometry of intermediate **2**) lies about 0.1 ± 0.2 eV above $Co^+ + C_2H_6$ (see above). This puts the C−C bond activation transition state about 0.4 ± 0.5 eV above the $Co^+ + C_2H_6$ asymptote.

There are two plausible pathways for forming **1** from $CoCH_2^+ + CH_4$. The first involves oxidative addition of the C−H bond to the Co^+ center to form intermediate **3** followed by α-H migration, Scheme 1. The second is a four-centered addition across the $Co^+{=}CH_2$ π bond. We note that if intermediate **3** were formed, then we might have expected to see products corresponding to thermoneutral hydrogen scrambling, e.g. $CoCHD^+$ and $CoCD_2^+$. These products should have been observed at energies corresponding to the height of the barrier, but were not. Additionally, analysis of the molecular orbital character of this reaction points to the four-centered transition state. The appropriate molecular orbital considerations have been discussed in detail for the analogous reactions of transition metal oxides, MO^+ with D_2[51,52] and CH_4,[52] as well as the interaction of $CoCH_2^+$ with D_2.[26] Our analysis in all of these cases suggested that the four-centered transition state was operative. We therefore conclude that interaction of $CoCH_2^+$ with methane should also form a four-centered transition state, in agreement with the calculation of HK. These authors calculate that the TS lies 0.87 eV above the $CoCH_2^+ + CH_4$ reactants, somewhat larger than the 0.29 ± 0.09 eV value

(47) Elkind, J. L.; Armentrout, P. B. *J. Phys. Chem.* **1987**, *91*, 2037. Armentrout, P. B. *Annu. Rev. Phys. Chem.* **1990**, *41*, 313.

(48) Taylor, J. R. *An Introduction to Error Analysis*; Oxford University: Mill Valley, 1982.

(49) Low, J. J.; Goddard, W. A., III *J. Am. Chem. Soc.* **1984**, *106*, 6928, 8321; **1986**, *108*, 6114, Low, J. J.; Goddard, W. A., III *Organometallics* **1986**, *5*, 609.

(50) The threshold for C−C bond activation was ~1 eV while the threshold for C−H bond activation was measured to be 0.47 ± 0.12 eV.

(51) Clemmer, D. E.; Aristov, N.; Armentrout, P. B. *J. Phys. Chem.* **1993**, *97*, 544.

(52) Chen, Y.-M.; Clemmer, D. E.; Armentrout, P. B. *J. Am. Chem. Soc.* **1994**, *116*, 7815.

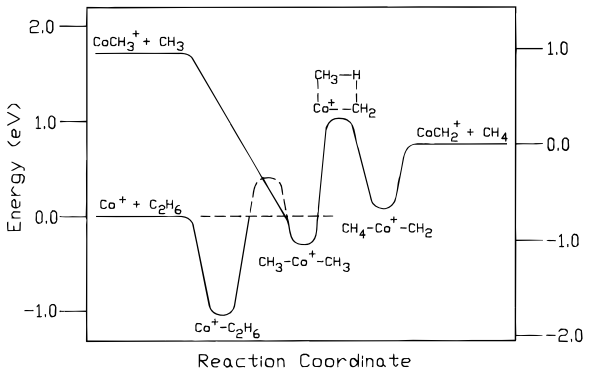

Figure 8. Potential energy surface for C−C bond activation in the interaction of $Co^+ + C_2H_6$.

measured here. We also note that this four-centered addition could occur with the carbon attached to the CH_2 carbon rather than to the metal, Figure 7. This would lead directly to the hydrido-ethyl−cobalt intermediate **2**, thereby providing a mechanism for production of CoH^+ and $CoC_2H_x^+$ products.

Bauschlicher *et al.*,[19] Musaev *et al.*,[20] Perry,[17] and HK[18] calculate that $CoCH_2^+$ has a $^3A_2$ ground state. Thus, the overall reaction of $CoCH_2^+ + CH_4$ to form Co^+ (^3F) + C_2H_6 (^1A) conserves spin. Musaev *et al.* assigned the electronic ground state ion configuration as $(3a_1)^2(1b_1)^2(1a_2)^1(2b_2)^2(4a_1)^2(5a_1)^1$. In this system, efficient C−H bond activation would occur if the ($5a_1$) acceptor orbital was empty and the ($1b_1$) donor orbital doubly occupied. Thus, the barrier to σ bond activation by $CoCH_2^+$ occurs because the acceptor orbital is singly occupied. The lowest lying state where the $5a_1$ orbital is empty is a $^1A_1$ state calculated to lie 1.28 eV higher in energy.[20] Reaction of this state of $CoCH_2^+$ with CH_4 in a spin allowed process would lead to production of $Co^+(^1D) + C_2H_6$, lying 1.44 eV above the ground state products.[39] Given these excitation energies, it seems unlikely that the transition state on the singlet surface would lie below that on the triplet surface, such that coupling between the singlet and triplet surfaces is probably not an important consideration for this reaction surface.

Given all this information, we can now construct a detailed potential energy surface for the demethanation of ethane, Figure 8. We use our value $D_0(Co^+-C_2H_6) = 1.04$ eV, Table 3, and the barrier height of 0.29 eV. The energy of the $(CH_4)CoCH_2^+$ intermediate could be estimated by simple bond additivity, namely $D_0(CoCH_2^+-CH_4) \approx D_0(Co^+-CH_4) = 0.93 \pm 0.06$ eV, Table 3. This is in reasonable agreement with the calculations of HK, who find $D_e(CoCH_2^+-CH_4) = 0.87$ eV.[18] It is possible that this bond is somewhat weaker, however, on the basis of comparing BDEs in similar complexes, $D_0(Co^+-H_2)$ and $D_e(CoCH_2^+-H_2)$. The latter BDE has been calculated[20] to be about half that measured for the former, Table 3.[13,53] Overall, we take the average of these two values to yield $D_0(CoCH_2^+-CH_4) \approx 0.67$ eV.

Given this potential energy surface, we can now rationalize our observations regarding demethanation of ethane and the reverse reaction. The forward reaction of $Co^+ + C_2H_6$ to form $CoCH_2^+ + CH_4$ has a threshold in excess of its endothermicity due to the barrier. No other C−C activation related products are directly affected by this barrier as their thresholds are higher in energy. For the reverse reaction, nothing is observed until energies above the barrier. The lowest energy process is formation of $Co^+ + C_2H_6$, but production of $CoCH_3^+ + CH_3$ becomes competitive as soon as it is thermodynamically allowed. This seems consistent with an appreciable barrier between $Co^+ + C_2H_6$ and the dimethyl intermediate **1**, otherwise ethane elimination should be much more efficient. Further, this suggests that the reverse reaction occurs mainly along the potential energy surface shown in Figure 8, rather than that shown in Figure 7, as the latter surface should also allow for efficient ethane elimination. The latter surface does provide a direct pathway for production of CoH^+ and $CoC_2H_4^+$ products in the $CoCH_2^+ + CH_4$ system. Overall, it appears that both pathways for methane elimination in the $Co^+ + C_2H_6$ system are accessible.

Coupling between C−C and C−H Bond Activation Processes. The reaction of $CoC_2H_4^+ + D_2$ forms $CoCH_2^+ + CH_2D_2$, $CoCH_2D^+ + CH_2D$, and $CoCHD^+ + CH_3D/CoCH_3^+ + CHD_2$ products. As there are no analogous processes in the reaction of $Co^+(C_2H_4)$ with Xe, these observations indicate that the C−H and C−C bond activation channels are connected to one another, although the coupling between these channels is inefficient based on the small cross section magnitudes of these channels. The mechanism for these processes is not obvious, but presumably involves the reverse of the dehydrogenation reaction along the potential energy surface shown in Figure 7 to form the $D-Co^+-CH_2CH_2D$ intermediate analogous to **2**, Scheme 1. A four-centered elimination would lead to $CoCH_2^+ + CH_2D_2$, Figure 7. As there should be a barrier to this process comparable to that for the four-centered transition state shown in Figure 8, it is not surprising that the observed threshold lies above the thermodynamic value.

Formation of the cobalt−methyl cation products from $CoC_2H_4^+ + D_2$ presumably involves conversion of intermediate **2** to **1**. This could occur via two mechanisms. Most probable is formation of the $Co^+(CH_2DCH_2D)$ adduct, which would lead to a $Co(CH_2D)_2^+$ intermediate that could form the $CoCH_2D^+$ product directly. Because we observe no isotope scrambling for the comparable dimethyl intermediate in the $CoCH_2^+ + CD_4$ system, this mechanism means that we should not observe any $CoCH_3^+$ or $CoCHD_2^+$ products in the $CoC_2H_4^+ + D_2$ reaction, consistent with observation. Another possible mechanism is an intermediate (or transition state) such as **3**, $(D)(CH_2D)$-$CoCH_2^+$, which would also be consistent with preferential formation of $CoCH_2D^+$. The former mechanism would also imply that $Co^+ + C_2H_6$ ($C_2H_4D_2$) should be observed as a product in the $CoC_2H_4^+ + H_2$ (D_2), albeit inefficiently. As discussed above, there is no unambiguous evidence for such a process, but neither can it be eliminated by the present data. Once the $Co(CH_2D)_2^+$ intermediate is formed, it can also eliminate either CH_2D_2 or CH_3D in an analogous four-centered process to that shown in Figure 8. This can explain the small amount of $CoCHD^+ + CH_3D$ observed and could contribute to the $CoCH_2^+ + CH_2D_2$ product channel as well.

Coupling of C−C and C−H bond activation processes are also observed in the reaction of $CoCH_2^+ + CH_4$ (CD_4). In this reaction, we see appreciable amounts of Co^+−hydride and small amounts of $CoC_2H_x^+$ products, suggesting that the reaction proceeds through the cobalt−hydrido ethyl ion intermediate **2**. Two mechanisms for this are possible. One, as noted above, is addition of the C-H bond across the $Co^+{=}CH_2$ π bond such that the carbon atoms bond to one another. As noted above, this has a measured barrier in excess of its endothermicity of 0.3−0.7 eV on the basis of the threshold for $Co^+(C_2H_4)$ product formation, reaction 29. In the CD_4 system, this pathway forms a $D-Co^+-CH_2CD_3$ intermediate, thereby explaining the 4:1 predominance of the CoD^+ product over CoH^+. The second mechanism involves formation of **1** followed by C−C bond coupling to form $Co^+(C_2H_6)$ [$Co^+(CH_2DCD_3)$] which can then react along the surface shown in Figure 7. This pathway should

(53) Haynes, C. L.; Armentrout, P. B. *Chem. Phys. Lett.* **1996**, *249*, 64.

yield a statistical 2:1 distribution of CoD^+ and CoH^+ products, in disagreement with our observations. The first mechanism is also more appealing as it provides a facile pathway for C−C bond coupling, which helps explain the much more efficient coupling between the C−H and C−C bond activation channels observed in this system compared with that found in the Co^+-(C_2H_4) + H_2 system.

Conclusions

In these experiments, we probe the potential energy surface (PES) for the activation of ethane by atomic Co^+ ions using guided-ion beam mass spectrometry. We are able to map out the $[CoC_2H_6]^+$ PES in detail by looking at the reactions of Co^+ + C_2H_6, TCA of $CoC_2H_6^+$, as well as the reverse of the dehydrogenation and demethanation reactions, $CoC_2H_4^+ + H_2$ (D_2) and $CoCH_2^+ + CH_4$ (CD_4), respectively. We directly measure a dehydrogenation barrier of 0.32 ± 0.12 eV and a demethanation barrier of 1.04 ± 0.11 eV (0.29 ± 0.09 eV in excess of its endothermicity). Lastly, we measure 0 K bond dissociation energies (BDEs) for $D_0(Co^+-C_2H_4) = 1.86 \pm 0.07$ eV and $D_0(Co^+-C_2H_6) = 1.04 \pm 0.05$ eV, in good agreement with literature values determined by other techniques. Although more speculative, $D_0(DCo^+-C_2H_4) = 1.13 \pm 0.16$ eV is also measured. By putting this information together with recent theoretical results, a quantitative potential energy surface for the $[CoC_2H_6]^+$ system is derived.

Acknowledgment. This work was supported by the National Science Foundation, Grant No. CHE-9221241. We thank Petra van Koppen, Max Holthausen, and Wolfram Koch for providing results before publication.

JA953769Y